International Journal of Scientific Research in Engineering and Management (IJSREM)
Volume: 09 Issue: 06 | June - 2025 SJIF Rating: 8.586 ISSN: 2582-3930

An Approach to Enhance the Tensile Properties of Friction Stir Welds using Teaching Learning Based Optimization

D.Vijayan

Department of Mechanical Engineering,

[a]Sri Chandrasekharendra Saraswathi Viswa Maha Vidyalaya, Enathur, Kanchipuram – 631561, Tamilnadu, India.

vijaiand2012@gmail.com

Abstract

In this paper, teaching and learning based optimization has applied to enhance the tensile properties of friction stir welding AA6061 and AA2024 aluminum alloys. Four significant variables were considered to conduct welding on age hardened aluminum alloys namely, tool rotational speed, welding speed, axial force, and tool pin profile. The effect of process variable on tool pin profile were analyzed by scanning electron micrographs, tensile testing, and elongation. The nugget zone is characterized by the onion rings whereas some of the weldments dealt with the defects such as cavities, tunnel, etc. TLBO algorithm has utilized to intend to minimize the defects by enhancing the tensile properties of the fabricated welds. From the experimental and algorithmic results, it is observed that the proposed RSM based TLBO approach is an effective approach for enhancing the tensile properties of fabricated age hardenable weldments.

Keywords: Tensile, Friction, welding, Response, TLBO, Tensile, Aluminum

1. Introduction

The growing focus on energy saving and environmental protection has increased the demand for light vehicles. Many advanced high-strength aluminum alloy sheets have been applied to auto parts to achieve the goal of reducing weight and improving crash resistance. In the past few years, various and multi-plate welding configurations have been used in the automotive industry. However, a weight reduction of more than 20-30% is unlikely, as it relies specifically on the use of aluminum sheets. Vehicle structures using aluminum alloys are an effective means of solving this problem, and there is a need for a method of joining dissimilar metals that is highly reliable and cost-effective. Aluminum and its alloys, are called non-metallic materials, which traditional welding techniques cannot give adequate strength because of porosity in the weld zone. Yet, ongoing advances in welding procedures and exploration by specialists have prompted the improvement of another welding technique called Friction Stir Welding (FSW).

Friction Stir Welding (FSW) is introduced as a solid-phase welding in 1991 by The Welding Institute (TWI), UK in 1991. Since FSW is solid phase welding, it has several advantages over traditional fusion welding methods, and solidification problems such as oxidation, shrinkage, porosity, and hydrogen solubility can be largely avoided, so FSW can be used in various industries such as aerospace, automotive, railway and marine [1-3]. This process consists of joining two fixed metals by mechanically mixing their edge zones with a rotary tool. The applied stirring causes external and internal friction within the workpiece, changing the state of the metal from solid to ductile, generating enough heat energy to maintain mixing and a Base plate for secure attachment of workpieces to be welded. Heat energy is considered to be one of the main factors determining defect formation and mechanical properties in friction stir welding. Many research investigations show the optimal heat input has attained by adjusting the FS Welding parameters to obtain adequate tensile properties of the weld joints. Song, Wang [4] concluded that the improvement in the quality of the FSW Al/Mg joint was implemented by setting up the heat input and the degree of mixing of the material. Huang, Meng [5] et al. was established that the FSW has superiority in the AL/Mg alloys, because it can limit the formation of IMC al-Mg due to the low peak temperature of the welding. However, IMCs still not maybe it is completely eliminated FSW, and the further increase of the joint strength thus is limited. In the welding process, it is assumed that the interaction of the tool and the material demonstrates the conditions of adhesion / sliding periodically. However, the lack of heat makes it difficult for the material to mix and causes irregular adhesion/sliding conditions. In addition, this lack of heat can lead to the formation of volumetric defects or

harmful tool failures. Liu, Xin [6] reported frictional heat played an important role in grain refinement. When there is insufficient heat or plastic deformation, the dynamic recrystallization experienced in TMAZ is incomplete. This changes in heat input along the weld lines causes changes in grain size. Fu, Qin [7] concluded that improving the FSW joint was achieved by setting the heat inputs and adjusting the amount of material combined. Ahmed, Nagesh [8] reported, tool rotational speed and welding speed decide enough heat input to weld so as to favorably affect the weld characteristics. It was found that the absence of heat inputs makes the material less flexible and stable, so that the interaction of the tool and material becomes unstable and unpredictable from an increase in the resistance of the material to the movement of the tool[9]. As reported by Suresh, Elango [10], during the welding process, assume that the interaction of tools and materials appear periodically under adhesion/sliding conditions. However, the lack of heat input can cause the material more difficult to stir and cause irregular adhesion/sliding conditions. In addition, the lack of heat input can cause a volumetric defect or tool failure.

Technology parameters, such as tool speed and feed rate, as well as geometric parameters, such as the height and shape of tool pins or collars, strongly influence the efficiency of weld joint. Different tool geometries result in improved different grain crystallization structures, which ultimately leads to variable weld strength depending on the type of geometry.

Increasing these parameters may affect both metal flow and heat generation due to friction forces. In other words, heat distribution can be considered as a bridge between the FSW parameters and the final mechanical properties of the weld. Therefore, it must be carefully controlled during the welding process. Due to the importance of this issue, a lot of research has been done in this area recently. To produce high quality joints, selecting the optimal set of welding parameters is challenging. Manufacturers and design engineers face many challenges when it comes to producing high-quality joints. However, no success was achieved, mainly due to the variability of the FSW parameters affecting heat input. Therefore, creating a parameter-dependent formula to measure the heat input improves the FSW performance.

The process of choosing the optimal technical parameters involves many trials and errors, which are expensive and time consuming. Modeling can be effectively accomplished using statistical techniques artificial neural networks, fuzzy logic, genetic algorithm and other AI based tools to determine weldability, welding assistance, temperature strain distribution, fracture properties [11, 12]. Chen, Li [13]. studied the effect of pin geometry on material flow during FSW. The effect of pin threads on FSW material flow was demonstrated quantitatively. Alipour Behzadi, Ranjbar [14] studied the mechanical properties and microstructure of Al7020-T6 at various rotation speeds. It is shown that mechanical properties, such as hardness and tensile strength in the stir zone (SZ), increase with increasing speed from 500 to 1400 rpm. The recent development of electron backscattering (EBSD) paves the way for a better appreciation of this amazing process. This method allows the calculation of various microscopic details on a large scale and therefore opens up a new dimension to microstructural studies. Moharami [15] studied the EBSD method to study the tribological properties of the FSPed Al-30Mg2Si alloy. The finest structure were found with an average grain size of 3.5 ± 1.2 lm in the three FSPed sample.

FSW involves mechanical clamps and a rotating tool equipped with a customized pin that provides a stirring action to change the state of metal from solid to plastic based on the production of enough heat energy. Since, the mixing and joining occurs by a rotating tool and its pin, therefore no further consumables are required. Though, several environmental and cost benefits are involved in FSW, the final weld quality is directly proportional to the heterogeneous mix-up of two materials by the tool and its corresponding pin. Thus, in the past decades a large number of investigations dedicatedly presented for the understanding, improvement of FSW tools and its pin profiles irrespective of materials to be welded[16-24]. However, most of them deal with metallurgical behaviors during FSW using heuristics approaches to get local optima in order to obtain a better weld quality.

In recent days, evolutionary algorithms introduced in FS welding for the process maximization or to minimize human fatigue and risk. Many evolutionary algorithms became popular in FSW especially for solving conflicting objectives easily. For instance the evolutionary algorithms such as Genetic Algorithm (GA)[25-28], Ant Colony Optimization (ACO) algorithm[29], Artificial Bee Colony (ABC) algorithm, Simulated Annealing (SA) algorithm[30-32], Biography-Based Optimization (BBO) [33], Particle Swarm Optimization (PSO) [34, 35], Sequential Quadratic Programming (SQP) algorithm[36, 37], etc. are widely utilized in FS welding. However, most of them have failed to predict global optima due

to increasing complexity in real manufacturing problems. Because, there are some specific user defined control parameters reasonably to be set for the searching such as population size, generation numbers, etc. Hence, they are finding the solution within the parametric boundary. Thus, the efforts must be continued to develop a feasible algorithm to discover a sound global optimum solution.

Teaching Learning Based Optimization (TLBO) algorithm is a novel meta-heuristic algorithm introduced by Venkata Rao et al[38-40], which is developed from the philosophy based on teaching – learning process and mimics the influence of a teacher in a class room on the specified output of learners or students. TLBO is a population-based meta-heuristic algorithm and it doesn't require any specific parameters as similar to swarm intelligence algorithms. In the past decade, TLBO algorithm has been successfully implemented by researchers in various fields such as medical imaging, phase changing materials, truss structures, etc.[41-44]. Even though numerous researches that explore significant improvement of TLBO, association of FSW for obtaining global optima has never been obtained.

2. Teaching learning optimization algorithm

The main aim of human life is to impart knowledge to future generations. As the evolution takes place, the knowledge transfer process happens widely through various modes via schools, colleges or universities. In such a way, Rao et al [38]. have proposed a novel algorithm inspired by the teaching learning process called "Teaching-Learning Based Optimization Algorithm (TLBO)". The algorithm is basically mimicking the classroom environment where the knowledge transfer usually occurs from the teacher to his/her students. There are two knowledge transfer modules in the TLBO algorithm namely teacher phase and learner phase. In the teacher phase, the knowledge is transferred to the students or learners whereas the knowledge transfers via interaction between the group of learners or students in the learner phase. When the learner who has potential knowledge in the subject, acts as teacher for his group members during the interaction process. The main aim of the knowledge transfer is to improve the marks / grades of the learners or students in the examination. Thus, in TLBO, the fitness function is considered as "result", and different process parameters involved in the welding process were considered as subjects for "population" of learners. The individual best fitness value is considered to be the teacher. The working phases of TLBO are discussed below,

2.1. Teacher phase:

As discussed, a group of learners or students learns a subject in teacher phase and the main objective of the teacher is to increase the mean results of the class in corresponding subject or his/her subject. The capacity of teacher depends on his/her capability or own knowledge. At iteration i, suppose there is 'n' learners (population size) who reads 'm' number of subjects (process variables). They have mean results M_{ji} in particular subject 'j'($j=1,2,3\ldots., m$). If 'K_{best}' is the best learner result, then overall best result will be 'X_{total} -$k_{best,i}$', considering all the subjects together obtained in the entire population of learners. It is assumed that the teacher has more knowledge of his/her subject as compare to the learners. Therefore, the best learner who is in the learning group has considered as a highly educated person or as a 'Teacher'. The difference between the existing mean result of each subject and the result of corresponding teacher for each subject is calculated as using the Equation 1:

$$Difference\_Mean_{j,k,i} = r_i(X_{j,kbest,i} - T_f M_{j,i}) \qquad \text{Equation 1}$$

Where, $X_{j,kbest,i}$ is the result of the best learner in subject j. T_F is the teaching factor in the range and r_i is the random number in the range [0, 1]. Usually the value of teaching factor T_f is decided using the following Equation 2.

$$T_F = round[1+rand(0,1)(2-1)] \qquad \text{Equation 2}$$

Then the teacher phase is updated according to the Equation 3, based on obtained results from equation 1.

$$X'_{j,k,i} = X_{j,k,i} + Difference\_Mean_{j,k,i} \qquad \text{Equation 3}$$

Where, $X'_{j,k,i}$is the updated value of $X_{j,k,i}$. $X'_{j,k,i}$ is accepted when converged to better function value. Toward the end of the teacher phase all the accepted function values are put away and these values become the input to the student phase. The student phase relies on the teacher phase.

2.2. Learner phase

Learners increase their knowledge by way of interaction with different learners within the class or group. In this interaction method there are no principles or any rules, therefore learners can have interaction arbitrarily with each other learner. Learner typically takes knowledge only from the other best learner, who has best knowledge when compared to him/her. Suppose 'A' and 'B' are two learners are arbitrarily selected, whose knowledge are not equal. So, the newest updated values may be estimated for the learning process is formulated using the Equation 4 for maximization problems.

$$X_{i,new} = \begin{cases} X_i + rand(X_i - X_j), if\ f(X_i < f(X_j) \\ X_i + rand(X_j - X_i), otherwise \end{cases}, \quad \textit{Equation 4}$$

Where X_j is the j^{th} learner different from X_i, and $f(x)$ is the objective function value of X, if $X_{i,new}$ is better than X_i, then accept $X_{i,new}$.

3. Experimental setup

Figure 1 shows the FSW setup used in the present investigation. Hot rolled AA2024 – T3 and AA6061-T6 aluminum alloys were used to prepare the weld specimen. The chemical composition of AA2024-T3 and AA6061-T6 are presented in Table 1. The dimensions of each AA2024 – T3 and AA6061 – T6 aluminum alloy is 300 × 150 × 6 mm were machined from the billets before subjecting to FSW. T3 indicates aluminum alloy is solution heat treated and cold worked whereas T6 stands for solution heat treated and artificially aged. And, all FSW tools were made by H13 hot work tool steel - is a versatile chromium-molybdenum steel used widely for hot work and cold work tooling operations. There are three FSW tool pin profiles were considered in the present investigation namely Cylindrical (1), Square (2) and Taper (3). Figure 2 shows the FSW tools used in the present investigation. The diameter of each tool shoulder and a pin is 18 mm and 6 mm respectively.

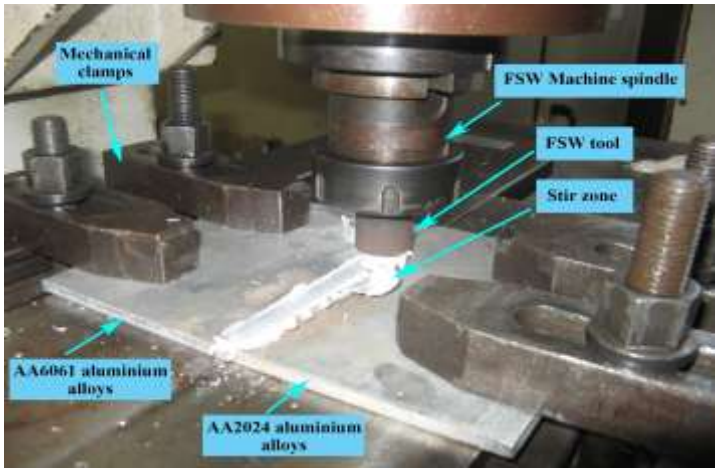

Figure 1 FSW setup

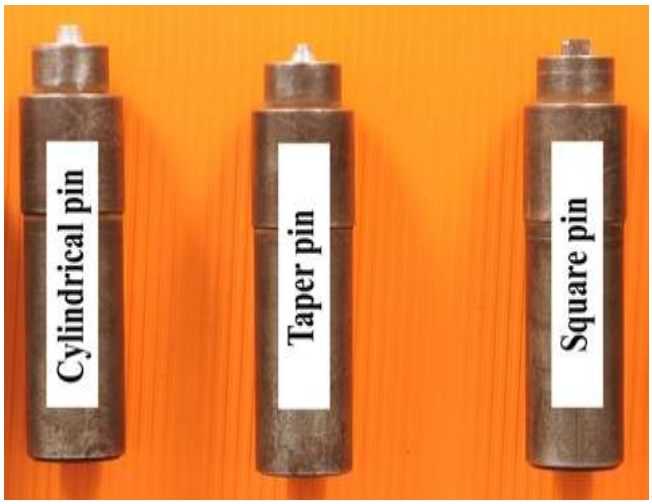

Figure 2 FSW Tools equipped with its pins

Table 1 Chemical composition of AA2024 – AA6061 aluminum alloys

Aluminum alloy (%)	Cr	Cu	Fe	Mg	Mn	Si	Tensile Yield Strength (MPa)	Elongation %
2024	0.10	4.90	0.90	1.80	0.90	0.50	324	20
6061	0.35	0.40	0.70	1.20	0.15	0.80	276	17

Table 2 Process parameters and their ranges

S.No	Process Parameters	Unit	Levels		
			-1	0	1
1	Tool rotational speed (X_1)	rpm	1350	1600	1850
2	Welding speed (X_2)	mm/min	30	60	90
3	Axial force (X_3)	kN	5	7	9
4	Pin profile (X_4)		1(Tap)	2(Squ)	3(Cyl)

RSM is a collection of mathematical and statistical technique is very useful to analyze and develop a mathematical model where a several factors influence the process. RSM is a reliable tool to correlate the relationship between the process factors and responses to establish a valid empirical model. The equation 5 represent the second order quadratic model is employed to indicate the responses,

Table 3 Design matrix and responses

Std	Run	Tool rotational speed (X_1)	Welding speed (X_2)	Axial force (X_3)	Tool pin profile (X_4)	Tensile Strength (TS) (N.Sq mm)	Percentage Elongation (PE) (%)
1	7	1350	30	7	2	107.075	9.735
2	8	1850	30	7	2	108.095	7.995
3	11	1350	90	7	2	108.085	10.215
4	5	1850	90	7	2	99.825	8.215
5	25	1600	60	5	1	120.934	11.145
6	3	1600	60	9	1	125.398	8.925
7	4	1600	60	5	3	116.324	10.135
8	22	1600	60	9	3	122.618	8.485
9	18	1350	60	7	1	120.648	10.025
10	28	1850	60	7	1	117.744	9.305
11	6	1350	60	7	3	118.894	9.865
12	30	1850	60	7	3	114.054	7.875
13	21	1600	30	5	2	106.105	10.325
14	14	1600	90	5	2	104.895	10.535
15	23	1600	30	9	2	114.994	8.795
16	17	1600	90	9	2	110.994	9.255

17	20	1350	60	5	2	117.204	11.045
18	29	1850	60	5	2	114.664	8.885
19	19	1350	60	9	2	120.968	9.025
20	27	1850	60	9	2	122.528	8.135
21	31	1600	30	7	1	114.004	9.435
22	16	1600	90	7	1	103.105	10.435
23	26	1600	30	7	3	109.035	8.685
24	13	1600	90	7	3	107.075	9.655
25	24	1600	60	7	2	134.861	10.875
26	15	1600	60	7	2	140.101	11.015
27	2	1600	60	7	2	135.671	10.885
28	12	1600	60	7	2	135.741	11.245
29	1	1600	60	7	2	136.371	11.215
30	10	1600	60	7	2	137.801	11.145
31	9	1600	60	7	2	139.761	11.295

$$Y = \beta_o + \sum_{i=1}^{k} \beta_i x_i + \sum_{i=1}^{k} \beta_{ii}^2 x_i^2 + \sum_{i<j} \beta_{ij} x_i x_j + \in$$ *Equation 5*

where βo is the average of responses and β_i, β_{ii}, and β_{ij} are the coefficients that depend on the respective main and interaction effects of the parameters, and Ɛ is a statistical error. There are two designs that are familiar in RSM namely central composite design (CCD) and Box-Behnken design (BBD). In the present investigation, BBD is considered to design the experiment. BB design will not have any points at the corners, because these are extreme conditions which are often hard to set, hence BB design is efficient moreover, few runs are made in this design matrix therefore an accurate quadratic model can be developed. Inappropriate welding parameters produce defects especially in SZ. Therefore, to produce defect free weld joints based on the thorough literatures survey each FS welding parameter and their corresponding levels are to be identified. The FSW experimental parameters and their levels followed in present investigation is presented in Table 2. Based on the BB design, four factors and three levels, therefore totally 31 experiments were chosen to organize the experiment. Thereafter, all the weld joints are fabricated and they were allowed for the metallographic and mechanical testing. All the fabricated FS welded samples were machined as per ASTM E407-09 standards with a dimension of 40 mm × 10 mm × 10 mm perpendicular to the welding direction using wire electrical discharge machining (WEDM) as presented in Figure 3. The microstructures of FS welded AA2024 – AA6061 aluminum alloy were analyzed using scanning electron microscope (Make: Quanta, Switzerland. Model: 3D FEG-I) to identify the weld defects and a computerized universal testing machine equipped with extensometer has operated with the cross-head speed of 1mm/min to understand the tensile behavior such as TS and its corresponding PE of the fabricated specimens. The results obtained from the TS with its corresponding PE is presented in Table 3.

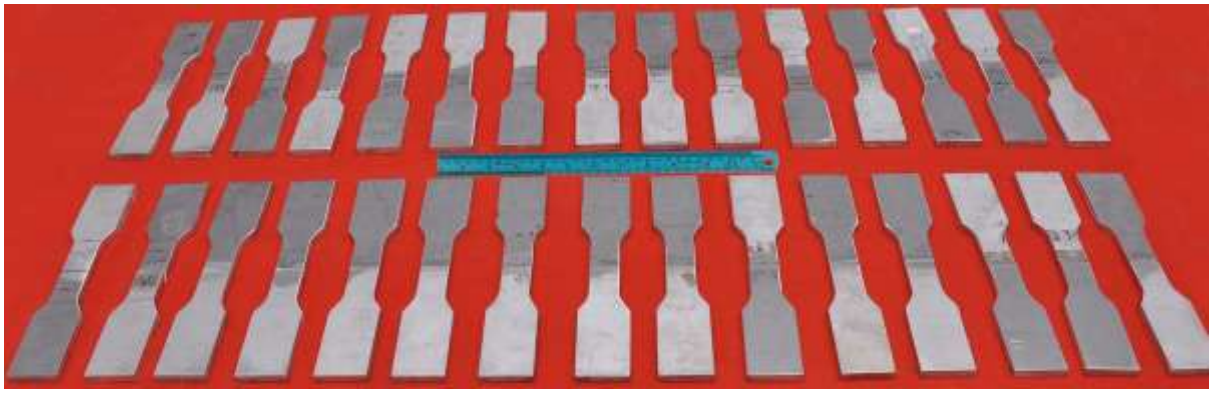

Figure 3 FS welded AA2024 – AA6061 aluminum alloys

Table 4 (a) ANOVA for tensile strength

Source	Sum of Squares	df	Mean Square	F - Value	p-value Prob > F	
Model	4136.541	14	295.467	96.954	< 0.0001	significant
X_1	21.238	1	21.238	6.969	0.0178	
X_2	53.460	1	53.460	17.542	0.0007	
X_3	116.396	1	116.396	38.194	< 0.0001	
X_4	15.945	1	15.945	5.232	0.0361	
$X_1 * X_2$	21.530	1	21.530	7.065	0.0172	
X1 * X3	4.203	1	4.203	1.379	0.2575	
X1 * X4	0.937	1	0.937	0.307	0.5869	
X2 * X3	1.946	1	1.946	0.639	0.4359	
X2 * X4	19.973	1	19.973	6.554	0.0210	
X3 * X4	0.837	1	0.837	0.275	0.6074	
X1^2	852.982	1	852.982	279.896	< 0.0001	
X2^2	2999.911	1	2999.911	984.384	< 0.0001	
X3^2	396.050	1	396.050	129.959	< 0.0001	
X4^2	506.492	1	506.492	166.199	< 0.0001	
Residual	48.760	16	3.047			
Lack of Fit	22.801	10	2.280	0.527	0.8231	not significant
Pure Error	25.959	6	4.327			
Cor Total	4185.301	30				
		R^2	0.9883	Adj R^2	0.9782	

Table 4(b) ANOVA for percentage elongation

Source	Sum of Squares	df	Mean Square	F - Value	p-value Prob > F	
Model	35.1261	14	2.5090	46.1801	< 0.0001	significant
X_1	7.5208	1	7.5208	138.4265	< 0.0001	
X_2	0.9296	1	0.9296	17.1106	0.0008	
X_3	7.4419	1	7.4419	136.9732	< 0.0001	
X_4	1.7404	1	1.7404	32.0335	< 0.0001	
$X_1 * X_2$	0.0169	1	0.0169	0.3111	0.5848	
X1 * X3	0.4032	1	0.4032	7.4217	0.0150	
X1 * X4	0.4032	1	0.4032	7.4217	0.0150	
X2 * X3	0.0156	1	0.0156	0.2876	0.5991	
X2 * X4	0.0002	1	0.0002	0.0041	0.9495	
X3 * X4	0.0812	1	0.0812	1.4950	0.2391	
X1^2	9.9592	1	9.9592	183.3065	< 0.0001	
X2^2	4.6939	1	4.6939	86.3940	< 0.0001	

X3^2	2.8740	1	2.8740	52.8979	< 0.0001	
X4^2	3.7478	1	3.7478	68.9809	< 0.0001	
Residual	0.8693	16	0.0543			
Lack of Fit	0.6910	10	0.0691	2.3255	0.1569	not significant
Pure Error	0.1783	6	0.0297			
Cor Total	35.9954	30				
		R^2	0.9758	Adj R^2	0.9547	

3.1. Formulation of optimization problem

The objective of the present investigation is to improve the tensile behavior of FS welded dissimilar AA2024 – AA6061 aluminum alloys by optimizing the process parameters namely tool rotational speed (X_1), welding speed (X_2), axial force (X_3) and tool pin profiles (X_4) such as such as Cylindrical (1), Square (2) and Taper (3). Therefore, the objective function can be formulated as follows,

Maximize, TS = f (X_1, X_2, X_3, X_4)

Maximize, PE = f (X_1, X_2, X_3, X_4)

Based on the objective function, the regression models have been developed for each response such as TS and PE by using Design expert v8. The developed regression model is presented in equation 6 and equation 7.

TS = -518.54492 +0.56203 * X(1) +3.08830 * X(2) +24.56809 * X(3) +29.54286 * X(4) -3.09333E-004 * X(1) * X(2) +2.05000E-003 * X(1) * X(3) -1.93580E-003 * X(1) * X(4) -0.011625 * X(2) * X(3) +0.074485 * X(2) * X(4) +0.22875 * X(3) * X(4) -1.74771E-004 * X(1)^2 -0.022761 * X(2)^2 -1.86078 * X(3)^2 -8.41716 * X(4)^2 *Equation 6*

PE = -39.50381 +0.055880 * X(1) +0.12439 * X(2) +0.60442 * X(3) +4.06361 * X(4) -8.66667E-006 * X(1) * X(2)+6.35000E-004 * X(1) * X(3) -1.27000E-003 * X(1) * X(4) +1.04167E-003 * X(2) * X(3) -2.50000E-004 * X(2) * X(4) +0.071250 * X(3) * X(4) -1.88848E-005 * X(1)^2 -9.00331E-004 * X(2)^2 -0.15851 * X(3)^2 -0.72405 * X(4)^2 *Equation 7*

Analysis of variance (ANOVA) is utilized to check the effect of the FSW parameters and their interactions on the response variable. Table 4(a) and Table 4(b) show the results of ANOVA at 95% confidence level for each TS and PE. The obtained R-Squared, Adj R-Squared values for TS and PE are 0.9883, 0.9758, 0.9782, 0.9547 respectively and the predicted R-Squared values are 0.9602 and 0.8827. The "Predicted R-Squared" values are closer and reasonable agreement with "Adj R-Squared" values for both TS and PE. Therefore, the model can be used to navigate the design space for further development of multi response optimization.

4. Results and discussion

Based on the empirical relationship developed, the effects of tool pin profile based on each parameter involved in FSW were plotted graphically using 3D surface plots. The normal probability plot for studentized residuals on TS and PE are plotted to understand the closeness of predicted results with experimental results. The developed normal probability plots for TS and PE are presented in Figure 4(a) and 4(b). It can be observed that the studentized residuals are very close to 45^O line, indicating the model has perfect fitness and the data follow the normal distribution, except three outliers.

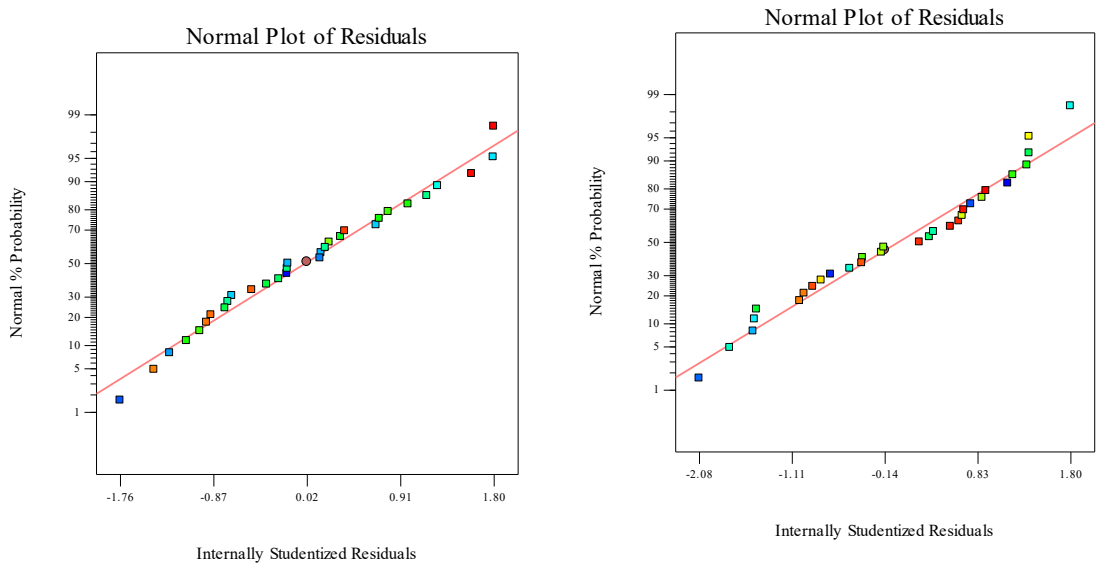

(a) (b)

Figure 4 Normal probability plot for (a). tensile strength, (b). percentage elongation

From the overall experiment, it can be observed that the rate of plastic flow of material, amount of heat generated and material mixing is entirely based on tool pin profiles. Therefore, the effects of each process parameters in the present investigation is discussed based on each tool pin profiles and their corresponding obtained results are presented graphically in Figure 5 - 7. From the 3D surface plots, it can be noticed that the TS of weld joints is lower than the base metals irrespective of process parameters. Very low or high levels of FSW process parameters produce low TS and PE in the fabricated AA2024-AA6061 aluminum alloy. As the combination of operating parameters increases frictional heat therefore which induces much material flow leads to precipitation growth, localization of strains and coarsening of grains in TMAZ, HAZ and SZ than the base metal.

4.1. Effects of tool pin profile

The tools equipped with square pin profile has higher TS and PE when compared to other tool pin profiles such as cylindrical and taper used in the present investigation. It was observed in most of the experimental runs, especially when using a square pin profile. Since, the rotating tools equipped with square pin profile has flat faces that produces pulsating effect which consequences more plastic flow as well as finer microstructure on the stir zone compared to other tool pin profiles[24, 29]. The tools equipped with taper pin profile produces lower TS and PE. Besides that, the tools equipped with cylindrical pin profile produces slightly higher TS and PE compared to taper pin profile.

4.2. Effects of rotational speed

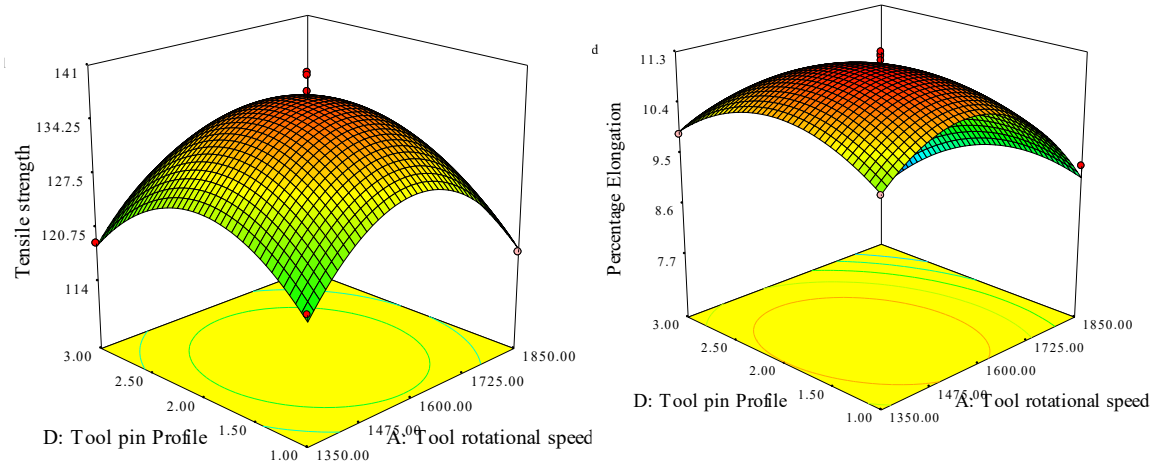

(a) (b)

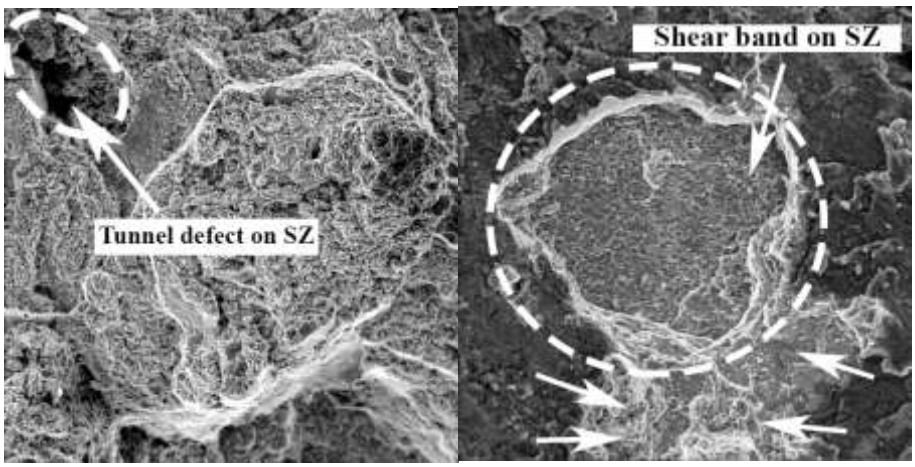

(c) (d)

Figure 5 Effect of tool rotational speed on (a). tensile strength, (b) percentage elongation, (c). tunnel defect on SZ and (d). shear band on SZ

The effect of tool rotational speed on TS and PE are presented in Figure 5(a) and 5(b). When the tool rotational speed is low (1300 rpm), or high (1850 rpm) the TS of fabricated dissimilar AA2024-AA6061 aluminum alloys is delivered with poor tensile strength. Due to inadequate heat input, the stirring action on the weld nugget is poor, which leads to a tunneling defect on the advancing side as presented in Figure 5(c). At rotational speed (1600 rpm), the tool provides an improved mixing that materializes a better interaction between the tool and a workpiece and reduces weld defects on the WN. Hence, TS of fabricated FS welded AA2024 – AA6061 aluminum alloys is increased. However, high tool rotational speeds induced shearing bands on the outer face layer particularly near HAZ due to high heat input. The developed shear bands on the outer layer is presented in Figure 5(d). Kouadri-Henni and Barrallier, Lee and Kwon claimed a similar observation on Al 6061/AZ31 Mg alloys welded by using FSW[45]. From the observations, it can be observed that the formation of the shear bands occurred mainly due to mass of material flow by penetration and gliding movements under the consequence of shoulder and pin. Shear bands are logically related with high strain energy leading to better chemical etching and seem as arcs. At last, it was quite observed that the thickness of the shear bands is more along the advancing side compared to the retreating side. On the other hand, increasing tool rotational speed improves the material flow in the NZ and TMAZ therefore an intense clustering of strengthening precipitates in NZ, TMAZ and HAZ and localization of strain decrease the PE of the fabricated FS welded joints.

4.3. Effects of welding speed

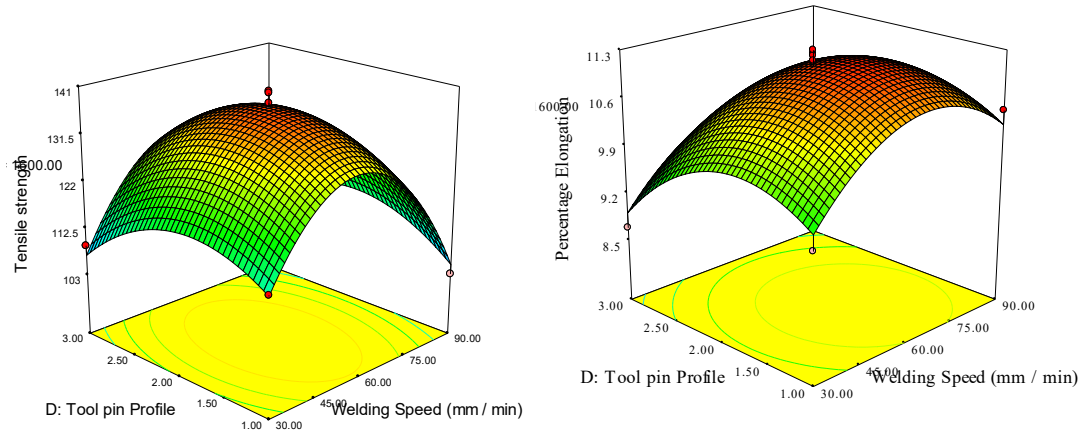

(a) (b)

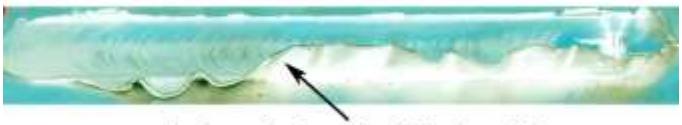

A schematic view of weld flash on SZ

(c)

Figure 6 Effects for welding speed on (a). tensile strength, (b). percentage elongation and (c) Weld flash on SZ

Figure 6(a) and 6(b) represent the effects of welding speed on TS and PE. It can be observed that, at lower level (30 mm/min) or higher level (90mm/min) FSW parameters produce low TS on fabricated AA2024-AA6061 aluminum alloys. This is due to insufficient friction heat and high frictional heat respectively. Low welding speed promotes the metallurgical transformations on the weld zone thus obtaining lower TS of the FS welded joints. Whereas at high welding speed, tool travels along weld lines faster thus discourages material stirring and flow of material causes reduction of localized heat input in the WN and vice versa. Hence, low TS was observed on the fabricated weld joints.

Moreover, the increase in the welding speed demoralizes the clustering effect of strengthening precipitates, plastic flow of materials and localization of strain. Subsequently, increase in the welding speed results in the increase of PE. Since, increasing welding speed induces faster heating and cooling which causes precipitates to coarsen, hence elongation is increased on the fabricated weld joints. Low welding speeds (30 mm/min) induce much heat therefore excessive materials softening on the SZ is a quite common phenomena in heat treatable alloys. This excessive material softening promotes slipping condition due to low friction between the tool and the contact surfaces of the material, resulting formation of flash as shown in Figure 6(c) in the SZ and leading to poor weld joint quality on the fabricated AA2024-AA6061 aluminum alloys. The similar observations were made by Li et al. 2015; Mohamed et al. 2015[46, 47] on FS welding of AA6061 and AA7075 aluminum alloys respectively.

4.4. Effects of axial force

Axial force is another dominating FSW parameter which is mainly influencing frictional heat generation, homogeneous microstructure, mechanical properties and for the preservation of plasticized material. Figure 7(a) and 7(b) reveals the effects of tool axial force on TS and PE. The TS of the fabricated weld joint is low when low axial force is applied. Since, at low axial force, frictional heat is low thereby leads to inadequate material stirring on the WN produces cavities and micro-voids as shown in Figure 7(c). High axial force induces high frictional heat and plunge depth creates a bulk material flow on the shoulder so which makes a probe to stir by inadequate material along an axis corresponding to the weld direction on the SZ encourages clustering of strengthening precipitates results decrease in PE of the fabricated weld joints. However, the excess layers of material flow create onion rings shaped on the SZ around the shoulder as shown in Figure 7(d). Therefore, increase in axial force, decrease the PE of the fabricated weld joints. The similar observations were made by Dawood et al. 2015; Dwivedi 2014; Rodriguez et al. 2015 [48-50] on FS welding of AA6061 aluminum alloys.

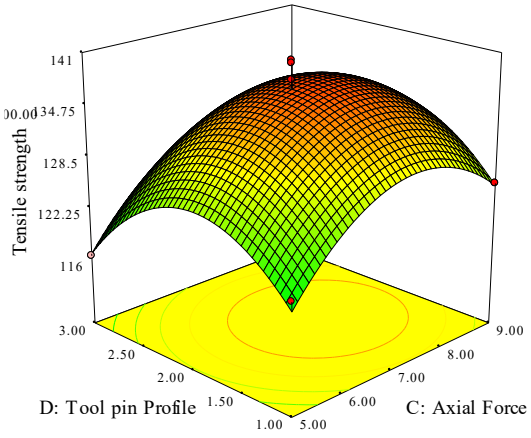

(a)

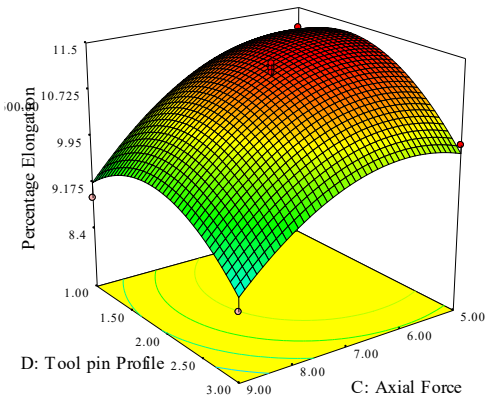

(b)

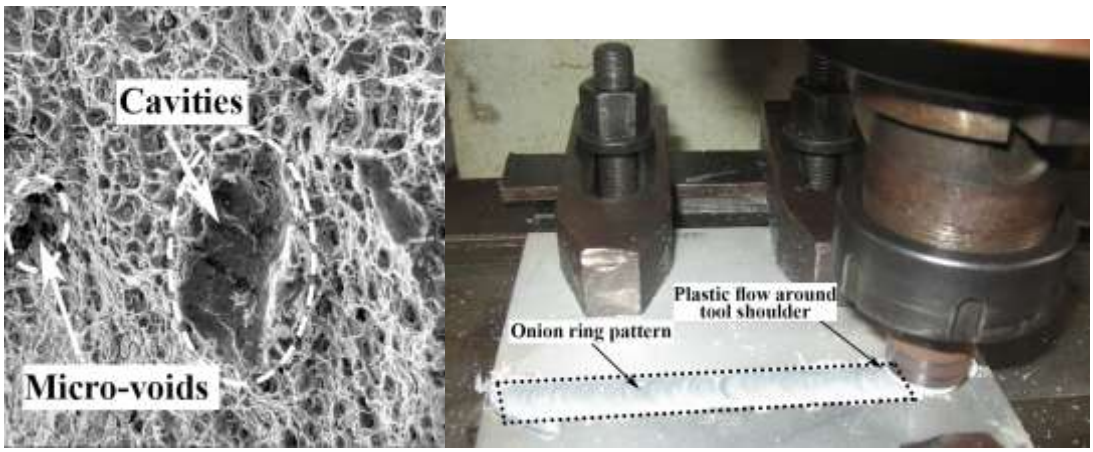

(c) (d)

Figure 7 Effects of axial force on (a). tensile strength, (b). percentage elongation, (c). Cavities and micro voids on SZ and (d). Onion ring pattern on the SZ

4.5. Multi response optimization using TLBO

The FS welding process factors such as tool rotational speed (X1), welding speed (X2), axial force (X3) and tool pin profiles (X4) such as Cylindrical (1), Square (2) and Taper (3) is used to determine the optimal process parameters in order to improve the tensile behavior of FS welded AA2024 – AA6061 aluminum alloys. To carry out the optimization process, the following fundamental steps in TLBO are to be followed. They are,

1. Generating initial populating learners
2. Estimating individual objective function and selecting best learners
3. Accepting best learner among other learners
4. Finding best teacher / learner and updating their knowledge
5. Estimating and accepting best objective function

The TLBO optimization algorithm has been performed by using MATLAB software. The population size, learner size and best learners in the algorithm for TLBO has been evaluated by conducting numerous trials. Figure 8 illustrates the flow chart of the TLBO algorithm. For the present investigation, a multi objective function (Z(TS+PE)) is developed and is represented in equation 7,

$$Z_{(TS+PE)} = \left[\frac{W_1 \times Z_{TS}}{Z_{TS-max}}\right] + \left[\frac{W_2 \times Z_{PE}}{Z_{PE-max}}\right] \qquad \textit{Equation 8}$$

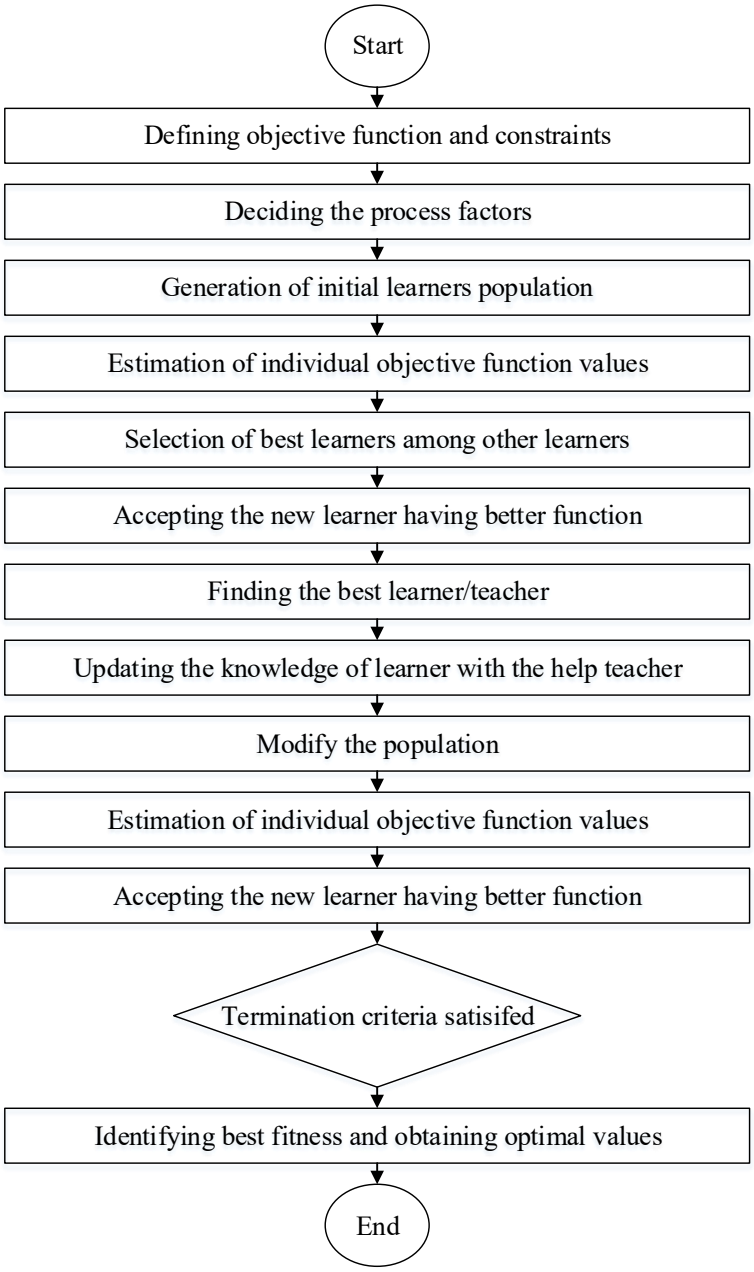

Figure 8 Flowchart of TLBO algorithm

Where, Z_{TS} and Z_{PE} are the developed regression models for TS and PE respectively. W_1 and W_2 are the weights for the function $Z_{TS\text{-}max}$ and $Z_{PE\text{-}max}$ respectively. $Z_{TS\text{-}max}$ and $Z_{PE\text{-}max}$ are the corresponding maximum values of TS and PE. The developed multi objective equation for FS welded dissimilar AA2024 and AA6061 aluminum alloys is presented in equation 8,

$$Z_{(UTS+TE)} = -(-6.043640468+0.007419314\times X(1)+0.016380499\times X(2)+0.031336293\times X(3)+0.31702963\times X(4)-1.36952e\text{-}06\times X(1)\times X(2)+2.06137e\text{-}05\times X(1)\times X(3)-6.1841e\text{-}05\times X(1)\times X(4)+0.00026623\times X(2)\times X(4)-2.21043E\text{-}06\times X(1)^2-0.000120611\times X(2)^2-0.00606369\times X(3)^2-0.061731696\times X(4)^2); \quad \textit{Equation 9}$$

The population of learners are considered as 25 for 4 subjects (FSW parameters). The operating range of parameters are,
1350 rpm $\leq X_1 \leq$ 1850 rpm
30 mm/min $\leq X_2 \leq$ 90 mm/min

$5kN \leq X_3 \leq 9kN$

$1 \leq X_4 \leq 3$ (Tool pin profiles: 1-Cylinder, 2-Square, 3-Taper), and the value of the teaching factor is considered as 2. All the above parameters have been considered based on the literature survey gathered and prior knowledge in the FSW. After considering all these parameters, the TLBO program in MATLAB has been run. After 100th iterations, optimal values of X_1, X_2, X_3 and X_4 are obtained at the objective function value ($Z_{(UTS+TE)}$) of 0.98569 and the values are 1658.60 rpm, 60.5512 mm/min, 5.4031kN and 1.8676 Ω 2 (Square) respectively. The obtained RSM based TLBO convergence plot and obtained FSW optimal parameters result is presented graphically in Figure 9(a) and 9(b).

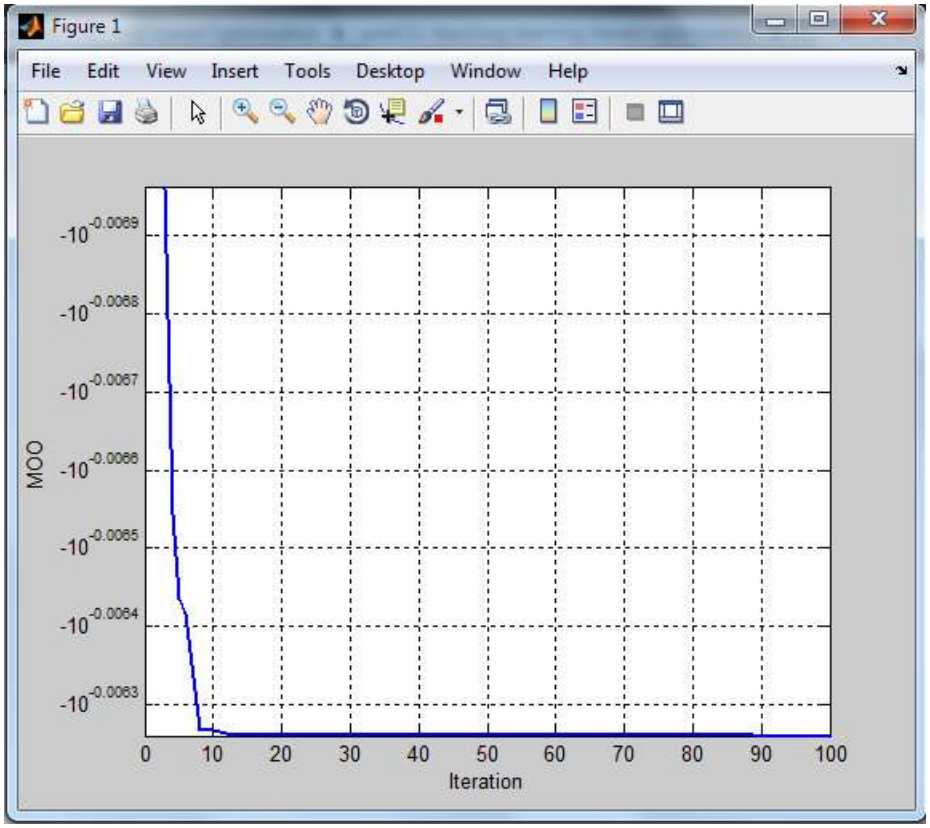

(a)

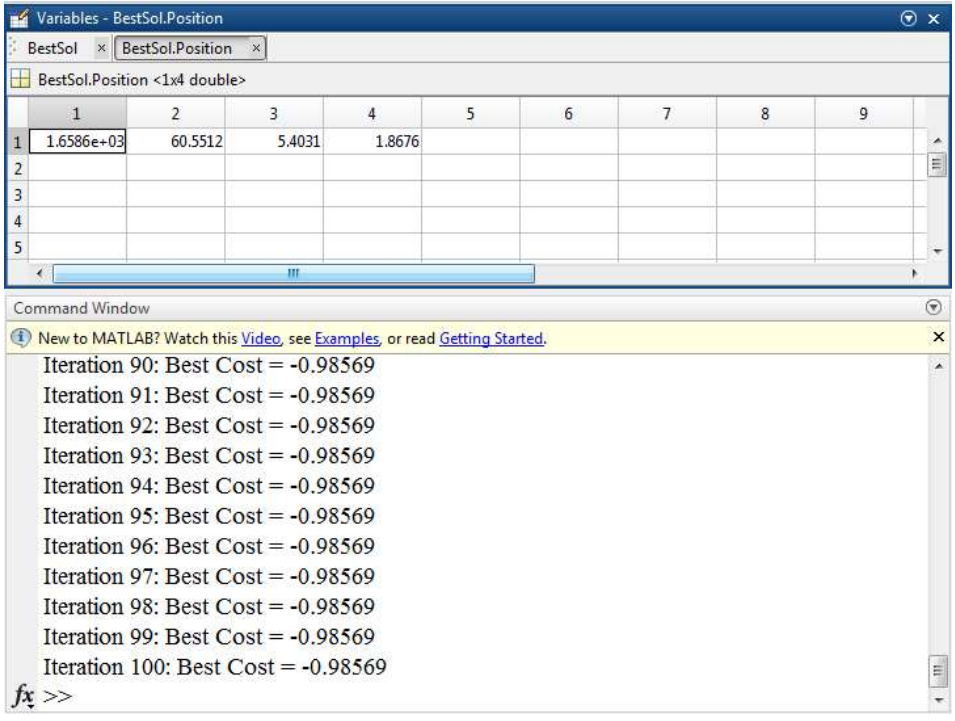

(b)

Figure 9 RSM based TLBO results of (a). Convergence plot, (b). FSW optimal parameters

5. Confirmation experiment

The optimal parameter obtained to achieve a maximum TS and PE of fabricated FS welded AA2024 – AA6061 aluminum alloys are validated further in order to demonstrate the effectiveness of the experiment and TLBO algorithm. Therefore, the experiment validation test has been carried out by using the obtained optimal parameter from the TLBO algorithm. The confirmation experiment results are tabulated in Table 5. The maximum TS of 145.745 MPa with its elongation of 13.45% is achieved on the fabricated FS welded dissimilar AA2024-AA6061 aluminum alloys.

Table 5 Confirmation experiment results

Tool rotational speed (X_1) (rpm)	Welding speed (X_2) (mm/min)	Axial force (X_3) (kN)	Tool pin profile (X_4)	Tensile strength (TS) (N/ Sq.mm)	Percentage elongation (PE) (%)
1658.60	60.5512	5.4031	1.8676Ω2	145.745	13.45

6. Conclusion

The multi response optimization using RSM based TLBO algorithm is used to improve the tensile behavior of FS welded AA2024 – AA6061 aluminum alloys. Four important FS welding process parameters considered for the present investigation namely tool rotational speed, welding speed, axial force and tool pin profiles such as cylindrical, square and taper. Totally 31 experiments were conducted using RSM based BB design. Based on the experiments conducted the following conclusions can be drawn,

1. High tool rotational speed provides an improved mixing that materializes a better interaction between the tool and a workpiece reduces weld defects on the WN thus increase TS on the fabricated weld joints whereas increasing tool rotational speed encourages clustering of strengthening precipitates thus reduces PE of the fabricated weld joints.
2. At high welding speed, tool travels along weld line faster so thus discourages material stirring and flow of material reduces localized heat input in the WN result low TS was observed whereas increase in the welding speed demoralizes the clustering effect of strengthening precipitates, plastic flow of materials and localization of strain. Therefore, increasing welding speed increases of PE of the fabricated weld joints.
3. At low axial force, frictional heat generated by the tool is low thereby leading to inadequate material stirring on the WN produces cavities and micro-voids. High axial force induces high frictional heat and plunge depth makes a bulk material flow on the shoulder so which makes a probe to stir by inadequate material along an axis corresponding to the weld direction on the SZ encourages clustering of strengthening precipitates results decrease in PE of the fabricated weld joints.
4. On the whole experimental runs, square tool pin profile plays a vital role and it is observed in most of the runs when tools are equipped with square pin profile. The pulsating effect on the rotating tool improves plastic flow on the stir zone which improves TS drastically when comparing other cylindrical and square tool pin profiles.
5. A multi objective regression modeling equations were developed by combining each single objective regression model equations of TS and PE of the dissimilar FS welded joints of aluminum alloys AA2024 and AA6061, and they are validated.
6. The optimal FSW parameters found by using RSM based TLBO algorithm such as tool rotational speed, welding speed, axial force and tool pin profile are 1658.60 rpm, 60.5512 mm/min, 5.4031kN and 1.8676 Ω 2 (Square) respectively.
7. An integrated RSM based TLBO is a very useful and effective approach on improving the TS and PE of the fabricated dissimilar FS welded joints of the AA2024-AA6061 aluminum alloys and they are validated.

Funding
The author(s) received no financial support for the research, authorship, and/or publication of this article.

References

1. Kumar, N., R.S. Mishra, and W. Yuan, *Friction Stir Welding of Dissimilar Alloys and Materials*. 2015: Elsevier Science.
2. Mishra, D., et al., *Friction Stir Welding for Joining of Polymers*, in *Strengthening and Joining by Plastic Deformation*. 2019. p. 123-162.
3. Rafiei, R., et al., *Dissimilar friction-stir lap-welding of aluminum-magnesium (AA5052) and aluminum-copper (AA2024) alloys: microstructural evolution and mechanical properties.* The International Journal of Advanced Manufacturing Technology, 2017. **94**(9-12): p. 3713-3730.
4. Song, Q., et al., *Improving joint quality of hybrid friction stir welded Al/Mg dissimilar alloys by RBFNN-GWO system.* Journal of Manufacturing Processes, 2020. **59**: p. 750-759.
5. Huang, Y., et al., *Friction stir welding/processing of polymers and polymer matrix composites.* Composites Part A: Applied Science and Manufacturing, 2018. **105**: p. 235-257.
6. Liu, D., et al., *Microstructure and mechanical properties of friction stir welded dissimilar Mg alloys of ZK60–AZ31.* Materials Science and Engineering: A, 2013. **561**: p. 419-426.
7. Fu, B., et al., *Friction stir welding process of dissimilar metals of 6061-T6 aluminum alloy to AZ31B magnesium alloy.* Journal of Materials Processing Technology, 2015. **218**: p. 38-47.
8. Ahmed, K.E., et al., *Studies on the effect of welding parameters for friction stir welded AA6082 reinforced with Aluminium Oxide.* Materials Today: Proceedings, 2020. **20**: p. 108-119.
9. Baratzadeh, F., et al., *Investigation of mechanical properties of AA6082-T6/AA6063-T6 friction stir lap welds.* Journal of Advanced Joining Processes, 2020. **1**.
10. Suresh, S., et al., *Sustainable friction stir spot welding of 6061-T6 aluminium alloy using improved non-dominated sorting teaching learning algorithm.* Journal of Materials Research and Technology, 2020. **9**(5): p. 11650-11674.
11. Mahto, R.P., et al., *A comprehensive study on force, temperature, mechanical properties and micro-structural characterizations in friction stir lap welding of dissimilar materials (AA6061-T6 & AISI304).* Journal of Manufacturing Processes, 2018. **31**: p. 624-639.
12. Liu, F.C., et al., *A review of friction stir welding of steels: Tool, material flow, microstructure, and properties.* Journal of Materials Science & Technology, 2018. **34**(1): p. 39-57.
13. Chen, G., et al., *Effects of pin thread on the in-process material flow behavior during friction stir welding: A computational fluid dynamics study.* 2018. **124**: p. 12-21.
14. Alipour Behzadi, M., et al., *Friction-stir-welded overaged 7020-T6 alloy joint: an investigation on the effect of rotational speed on the microstructure and mechanical properties.* International Journal of Minerals, Metallurgy, and Materials, 2019. **26**(5): p. 622-633.
15. Moharami, A., *High-temperature tribological properties of friction stir processed Al-30Mg2Si composite.* Materials at High Temperatures, 2020. **37**(5): p. 351-356.
16. Yang, M., et al., *Thermo-mechanical interaction between aluminum alloy and tools with different profiles during friction stir welding.* Transactions of Nonferrous Metals Society of China, 2019. **29**(3): p. 495-506.
17. Raturi, M., A. Garg, and A. Bhattacharya, *Joint strength and failure studies of dissimilar AA6061-AA7075 friction stir welds: Effects of tool pin, process parameters and preheating.* Engineering Failure Analysis, 2019. **96**: p. 570-588.
18. Entringer, J., et al., *The effect of grain boundary precipitates on stress corrosion cracking in a bobbin tool friction stir welded Al-Cu-Li alloy.* Materials Letters: X, 2019. **2**.
19. Chen, G., et al., *Three-dimensional thermal-mechanical analysis of retractable pin tool friction stir welding process.* Journal of Manufacturing Processes, 2019. **41**: p. 1-9.

20. Zhao, S., et al., *Effects of tool geometry on friction stir welding of AA6061 to TRIP steel.* Journal of Materials Processing Technology, 2018. **261**: p. 39-49.
21. Yang, C., et al., *A comparative research on bobbin tool and conventional friction stir welding of Al-Mg-Si alloy plates.* Materials Characterization, 2018. **145**: p. 20-28.
22. Sun, Z., C.S. Wu, and S. Kumar, *Determination of heat generation by correlating the interfacial friction stress with temperature in friction stir welding.* Journal of Manufacturing Processes, 2018. **31**: p. 801-811.
23. Mastanaiah, P., A. Sharma, and G.M. Reddy, *Role of hybrid tool pin profile on enhancing welding speed and mechanical properties of AA2219-T6 friction stir welds.* Journal of Materials Processing Technology, 2018. **257**: p. 257-269.
24. Hou, W., et al., *Dissimilar friction stir welding of aluminum alloys adopting a novel dual-pin tool: Microstructure evolution and mechanical properties.* Journal of Manufacturing Processes, 2018. **36**: p. 613-620.
25. Kamal Babu, K., et al., *Parameter optimization of friction stir welding of cryorolled AA2219 alloy using artificial neural network modeling with genetic algorithm.* The International Journal of Advanced Manufacturing Technology, 2017. **94**(9-12): p. 3117-3129.
26. Sreenivasan, K.S., S. Satish Kumar, and J. Katiravan, *Genetic algorithm based optimization of friction welding process parameters on AA7075-SiC composite.* Engineering Science and Technology, an International Journal, 2019.
27. Boukraa, M., et al., *Friction stir welding process improvement through coupling an optimization procedure and three-dimensional transient heat transfer numerical analysis.* Journal of Manufacturing Processes, 2018. **34**: p. 566-578.
28. Gupta, S.K., et al., *Experimental modelling and genetic algorithm-based optimisation of friction stir welding process parameters for joining of dissimilar AA5083-O and AA6063-T6 aluminium alloys.* 2018. **56**(3): p. 253-270.
29. Yang, X., et al., *Fatigue behaviors prediction method of welded joints based on soft computing methods.* Materials Science and Engineering: A, 2013. **559**: p. 574-582.
30. Babajanzade Roshan, S., et al., *Optimization of friction stir welding process of AA7075 aluminum alloy to achieve desirable mechanical properties using ANFIS models and simulated annealing algorithm.* The International Journal of Advanced Manufacturing Technology, 2013. **69**(5-8): p. 1803-1818.
31. Rambabu, G., et al., *Optimization of friction stir welding parameters for improved corrosion resistance of AA2219 aluminum alloy joints.* Defence Technology, 2015. **11**(4): p. 330-337.
32. Padmanaban, R., et al., *Simulated Annealing Based Parameter Optimization for Friction Stir Welding of Dissimilar Aluminum Alloys.* Procedia Engineering, 2014. **97**: p. 864-870.
33. Tamjidy, M., et al., *Multi-Objective Optimization of Friction Stir Welding Process Parameters of AA6061-T6 and AA7075-T6 Using a Biogeography Based Optimization Algorithm.* Materials (Basel), 2017. **10**(5).
34. Shojaeefard, M.H., et al., *Modelling and Pareto optimization of mechanical properties of friction stir welded AA7075/AA5083 butt joints using neural network and particle swarm algorithm.* Materials & Design, 2013. **44**: p. 190-198.
35. Zhang, Q., et al., *Multiobjective optimal design of friction stir welding considering quality and cost issues.* 2015. **20**(7): p. 607-615.
36. Kim, W.-k., B.-c. Goo, and S.-t. Won, *Optimal Design of Friction Stir Welding Process to Improve Tensile Force of the Joint of A6005 Extrusion.* Materials and Manufacturing Processes, 2010. **25**(7): p. 637-643.
37. Jung, S.P., T.W. Park, and Y.G. Kim, *Fatigue strength optimisation of friction stir welded A6005-T5 alloy sheets.* Science and Technology of Welding and Joining, 2013. **15**(6): p. 473-478.
38. Rao, R.V., V.J. Savsani, and D.P. Vakharia, *Teaching–learning-based optimization: A novel method for constrained mechanical design optimization problems.* Computer-Aided Design, 2011. **43**(3): p. 303-315.
39. Rao, R.V. and K.C. More, *Optimal design of the heat pipe using TLBO (teaching–learning-based optimization) algorithm.* Energy, 2015. **80**: p. 535-544.
40. Rao, R.V. and V. Patel, *An elitist teaching-learning-based optimization algorithm for solving complex constrained optimization problems.* international journal of industrial engineering computations, 2012. **3**(4): p. 535-560.

41. Singh Gill, H., et al., *Teaching-learning-based optimization algorithm to minimize cross entropy for Selecting multilevel threshold values.* Egyptian Informatics Journal, 2019. **20**(1): p. 11-25.
42. Venkata Rao, R. and V.D. Kalyankar, *Parameter optimization of modern machining processes using teaching–learning-based optimization algorithm.* Engineering Applications of Artificial Intelligence, 2013. **26**(1): p. 524-531.
43. Baby, R. and C. Balaji, *Thermal optimization of PCM based pin fin heat sinks: An experimental study.* Applied Thermal Engineering, 2013. **54**(1): p. 65-77.
44. Degertekin, S.O. and M.S. Hayalioglu, *Sizing truss structures using teaching-learning-based optimization.* Computers & Structures, 2013. **119**: p. 177-188.
45. Kouadri-Henni, A. and L. Barrallier, *Mechanical Properties, Microstructure and Crystallographic Texture of Magnesium AZ91-D Alloy Welded by Friction Stir Welding (FSW).* Metallurgical and Materials Transactions A, 2014. **45**(11): p. 4983-4996.
46. Mohamed, M.A., Y.H.P. Manurung, and M.N. Berhan, *Model development for mechanical properties and weld quality class of friction stir welding using multi-objective Taguchi method and response surface methodology.* Journal of Mechanical Science and Technology, 2015. **29**(6): p. 2323-2331.
47. Li, D., et al., *Investigation of stationary shoulder friction stir welding of aluminum alloy 7075-T651.* 2015. **222**: p. 391-398.
48. Dawood, H.I., et al., *The influence of the surface roughness on the microstructures and mechanical properties of 6061 aluminium alloy using friction stir welding.* 2015. **270**: p. 272-283.
49. Dwivedi, S.P.J.J.o.m.s. and technology, *Effect of process parameters on tensile strength of friction stir welding A356/C355 aluminium alloys joint.* 2014. **28**(1): p. 285-291.
50. Rodriguez, R., et al., *Microstructure and mechanical properties of dissimilar friction stir welding of 6061-to-7050 aluminum alloys.* 2015. **83**: p. 60-65.